สัมมนาวิชาการวิศวกรรมเครื่องกลแห่งประเทศไทยครั้งที่ 13
2-3 ธันวาคม 2542 โรงแรมรอยัลคลิฟบีชรีสอร์ท พัทยาใต้ ชลบุรี

Flying Characteristic Simulation of the Plane Wedge Type Slider Head and Rigid Disk in Magnetic Storage System

M.Mongkolwongrojn , S.Kwankaomeng
Electro-Mechanical Engineering Laboratory ReCCIT Faculty of Engineering KMIT'L
Chaloongkrung Road, Ladkrabang, Bangkok 10520
Tel 3269987 ext. 103 , Tel 3266053-101 ext. 2345
E-mail:kmmongko@kmitl.ac.th, E-Mail:sudaratk@hotmail.com

Abstract

This paper reports on the investigations of static and dynamic characteristics of self acting air bearing head and rigid disk in magnetic storage system. In order to consider the plane wedge type slider, which compose of two rails to pressurize the air. The design of ultra low clearance between head and rigid disk interface is to obtain high data storage density. Two degree of freedom motion of slider head; translation perpendicular to the disk surface and rotation around the transverse axis were simplified in this investigation. Numerical solution of the two dimensional nonlinear time variable modified Reynolds equation with slip flow effect has been formulated by using variable grid size. A numerical scheme base on the finite difference technique and iteration method have been used to simulate steady state flying characteristics. For dynamic characteristics, the Laplace transform is applied. The pressure distribution, flying height, loads, pivot position and spring and damping coefficient were obtained in this calculation.

1. Introduction

For rigid magnetic disk drive, The increased in memory capacity and higher reliability are strongly desired. To increase the storage density of the drives, it is essential to reduce the flying heights of their sliders (the gap between magnetic recording heads and disks). In current drives, the flying heights have been reduce to the 100 to 200 nm. range. On the other hand, to ensure higher drive reliability, contact between the sliders and the disks must be avoided. To meet this requirement, both lower and more stable flying heights of the sliders must be achieved.

Since the rotating disk vibrations consist of the first mode of several tens of microns and the higher order modes, it is not important only to predict the static characteristic but also to design the flying head slider with good compliance to disk vibration.This analysis included slip flow effects make it possible to evaluate submicron spacings.

In currently available contact-start-stop type flying head sliders, the load spring force must be sufficiently small (commonly about 100 mN) from the view points of flying head slider and disk wear. An air bearing with high degree of stiffness is required to keep the spacing variation between recording head and recording medium small. The conventional light load slider, however, has an upper limit of stiffness, because the air film stiffness decreases with decrease of the positive pressure of the air film, which is balanced by the load spring force. The slider can be simplified as show in Figure 1

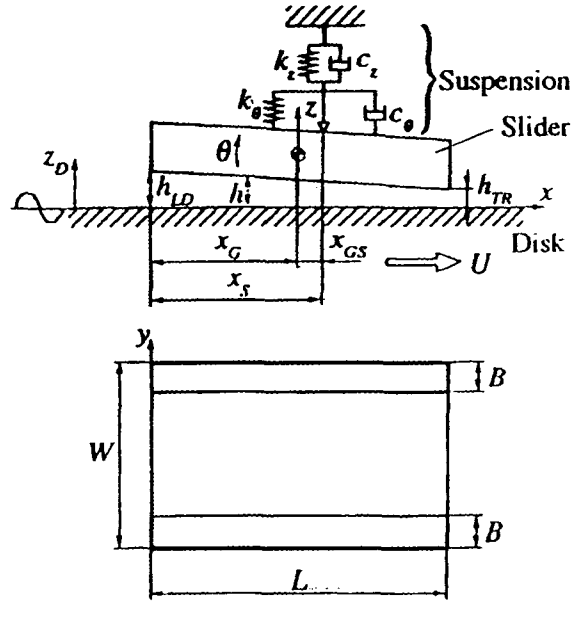

Fig.1 Analytical model of magnetic head slider

2.Theoretical Analysis

2.1 Generalized Reynolds Equation

To derive the air bearing equation, we adopt a rectangular coordinate system (x,y) with the origin placed at the corner of the inner and leading edges and with the x and y axes pointed in the slider's length and width direction respectively. Under the assumptions of negligible inertial and body force, molecular slip flow between the vary small gas film thickness, compressible. Reynolds equation, which governs the pressure distribution between the slider and disk can be written in dimensional form as

$$\frac{\partial}{\partial x}\left[ph^3\frac{\partial p}{\partial x}\right]+\frac{\partial}{\partial y}\left[ph^3\frac{\partial p}{\partial y}\right]=6U\mu\frac{\partial}{\partial x}[ph] +6V\mu\frac{\partial}{\partial y}[ph]+12\mu\frac{\partial}{\partial t}[ph] \tag{1}$$

where p is pressure, h is the local slider-disk separation, μ is the viscosity of the air; U and V are the sliding velocities in x and y direction.

When the gas between the slider and the rigid disk is assumed to be isothermal, the modified Reynolds equation considering molecular slip flow effects can be written in a nondimensional form as follows.

$$\frac{\partial}{\partial x}\left\{PH^3\left(1+\frac{6K_0}{PH}\right)\frac{\partial P}{\partial X}\right\}=\left(\frac{L}{B}\right)^2\frac{\partial}{\partial Y}\left\{PH^3\left(1+\frac{6K_0}{PH}\right)\frac{\partial P}{\partial Y}\right\} =\Lambda_X\frac{\partial(PH)}{\partial X}+\Lambda_Y\frac{\partial(PH)}{\partial Y}+\sigma\frac{\partial(PH)}{\partial T} \tag{2}$$

Here $\left(1+\frac{6K_0}{PH}\right)$ is the nondimensional pressure flow rate or Poiseuille flow factor. Using the nondimensionalized variables as

$$P=\frac{p}{p_a},H=\frac{h}{h_m},T=\omega t,X=\frac{x}{L},Y=\frac{y}{B}$$

where p_a = atmospheric pressure; h_m = minimum separation height; L = length of slider; B = width of slider; and ω = angular velocity of disk.

$\Lambda_x=\frac{6\mu UL}{p_a h_m^2}$ and $\Lambda_y=\frac{6\mu UB}{p_a h_m^2}$ are the bearing numbers in the x and y direction, respectively.

$\sigma=\frac{12\mu\omega L^2}{p_a h_m^2}$ is the squeeze number. Here μ is the viscosity of the gas, and U and V are the sliding velocities in the x and y directions, respectively. ; $K_0=\frac{\lambda_a}{h_m}$,K_0 is the Knudsen number and λ is the mean free path of the gas molecules.

2.2 Equation of motion

The dynamic characteristics of sliders are analyzed using the two-degrees-of-freedom model has typically been calculated by simultaneously solving the modified Reynolds equation with the force and moment balances that govern the motion of the air bearing slider flying over a rotating disk are

$$m\frac{d^2Z}{dt^2}+k_Z Z+F=\int(p-p_a)dA \tag{3}$$

$$I_0\frac{d^2\theta}{dt^2}+k_\theta\theta+M_\theta=\int(p-p_a)(x_g-x)dA \tag{4}$$

Using normalized form:

$$M_Z\ddot{Z}+F_S=\int_0^1\int_0^1(P-1)dXdY \tag{5}$$

$$I_\theta\ddot{\theta}+M_S-F_S X_{GS}=\int_0^1\int_0^1(P-1)(X_G-X)dXdY \tag{6}$$

where

$$F_S=F_0+K_Z(Z-X_{GS}\theta)+C_Z(\dot{Z}-X_{GS}\dot{\theta}) \tag{7}$$

$$M_S=M_0+K_\theta\theta+C_\theta\theta \tag{8}$$

2.3 The load carrying Capacity

The hydrodynamic force W will be computed by integrating the film pressure. The load carrying capacity of a slider bearing is given by

$$W=\int_0^1\int_0^1(P-1)dXdY \tag{9}$$

which adopted the trapezoid rule method to compute. To increase the accuracy of approximation of the load carrying capacity, fine finite difference mesh is needed, especially within the zones where the rate of change of pressure is large, such as around the trailing edge.

2.4 The pivot position

The coordinates of gas film center of pressure are

$$\bar{X}=\frac{1}{W}\int_0^1\int_0^1 X(P-1)dXdY \tag{10}$$

$$\bar{Y}=\frac{1}{W}\int_0^1\int_0^1 Y(P-1)dXdY \tag{11}$$

The net load and centers of pressure which appear in equation (9),(10) and (11) provide integral coupling of the pressure to the slider excursion.

2.5 The stiffness and damping coefficient

The stiffness $K_{m,n}$ and damping coefficient $C_{m,n}$ are obtained by the following integrations

$$K_{11} + j\omega C_{11} = -\frac{p_a b l}{h_0}\int_0^1\int_0^1 G_1 dXdY \tag{12}$$

$$K_{12} + j\omega C_{12} = -\frac{p_a b l^2}{h_0}\int_0^1\int_0^1 G_2 dXdY \tag{13}$$

$$K_{21} + j\omega C_{21} = -\frac{p_a b l^2}{h_0}\int_0^1\int_0^1 G_1 (X_G - X) dXdY \tag{14}$$

$$K_{22} + j\omega C_{22} = -\frac{p_a b l^3}{h_0}\int_0^1\int_0^1 G_1 (X_G - X) dXdY \tag{15}$$

3. Numerical Analysis Method

3.1 Static characteristic

Static pressure distribution can be obtain by solving equation (2) without the time dependent term. The steady-state nonlinear modified Reynolds equation is expressed as

$$\begin{aligned}&\frac{\partial}{\partial X}\left(\left(1+\frac{6K_0}{PH}\right)PH^3\frac{\partial P}{\partial X}\right)+\\&\left(\frac{L}{B}\right)^2\frac{\partial}{\partial Y}\left(\left(1+\frac{6K_0}{PH}\right)PH^3\frac{\partial P}{\partial Y}\right)\\&-\Lambda_X\frac{\partial}{\partial X}(PH)-\Lambda_Y\frac{\partial}{\partial Y}(PH)=0\end{aligned} \tag{16}$$

can be solved by finite difference and linearized Taylor series approximation equation is

$$f(P) \cong f(P_0) + (P - P_0) f'(P) \tag{17}$$

Solving equation(16) iteratively until ΔP converge to zero, which fixed air film thickness with the boundary conditions are

$$P(0,Y) = P(1,Y) = P(X,0) = P(X,1) = 1 \tag{18}$$

3.2 Dynamic characteristic

To calculate the dynamic flying characteristics of slider, Laplace transformation of the equation of dynamic components (ΔP and ΔH) can be solved with boundary value in pressure P_s and pressure fluctuation function as:

$$P(X,Y,T) = P_s(X,T) + \Delta P(X,Y,T) \tag{19}$$

$$H(X,T) = H_S(X) + \Delta H(X,T) \tag{20}$$

$$Z(T) = Z_S + \Delta Z(T) \tag{21}$$

$$\theta(T) = \theta_S + \Delta\theta(T) \tag{22}$$

The resulting pressure flutuation is expressed as equation (23) where the slider motion is retricted to two degrees of freedom

$$\Delta P = G_1 Z + G_2\theta_p + G_3 Z_1 \tag{23}$$

Where G_1, G_2 and G_3 correspond to the bouncing mode, pitching mode and disk surface oscillation, respectively. Both the bearing stiffness and damping coefficients of the air bearing are calculated be integrating the G_1, G_2 and G_3 functions.

Displacement of the disk is Z_1, so the fluctuation of slider spacing is expressed as

$$\Delta H = Z - Z_1 + \theta_p(X_G - X) \tag{24}$$

The boundary condition are expressed by

$$\Delta P(0,Y,T) = \Delta P(1,Y,T) = \Delta P(X,0,T) = \Delta P(X,1,T) = 0 \tag{25}$$

4. Numerical Simulation Result

Simulation of the flying characteristics of the Plane wedge type slider were made for both static and dynamic conditions. In cases, the slider geometry as shown on Fig.1, dimension of slider is composed of slider length (SL=4.05 mm.) and slider rail width (SB=0.5 mm.).The applied load was 0.147 Newton.

4.1 Static characteristics

4.1.1 Static pressure distribution are presented on Fig.2.and Fig.3 respectively. The equilibrium slider pitch angle is 0.0001 radian and the clearance at trailing edge is 0.142 μ m. Along the rail, the air is pressurized due to the wedge effect. This pressure is increases toward the trailing edge due to the positive pitch angle of slider and then decreases suddenly at trailing edge because of side leakage. Effect of high bearing number on the pressure distribution is shown in Fig. 3 for minimum spacing of 0.1 μ m. It is seen that varying bearing number due to vary the disk speed causes the pressure distribution and the peak pressure to increase.

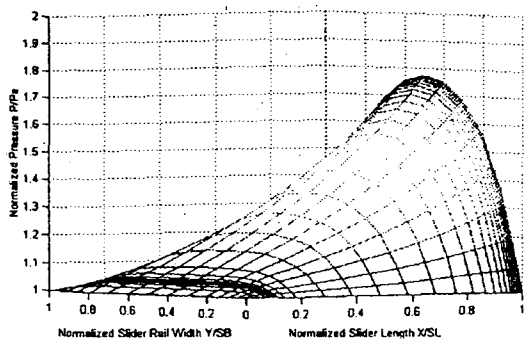

Hm=0.1um.,U=30 m/s, bn= 13025.57

Fig.2 Pressure distributions profile

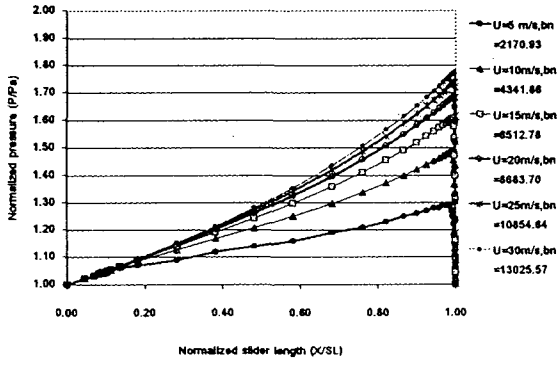

Fig.3 Static pressure at the middle of the rail, Hm=0.1 um.

4.1.2 Air film thickness

A desired characteristic of a slider used in magnetic recording is to experience only small variations in flying height as the slider is accessed to different radial location over the disk surface and avoid metal contact. On Fig.4 is presented the relationship of the nondimensional fly height along the slider rail with varying minimum film thickness.

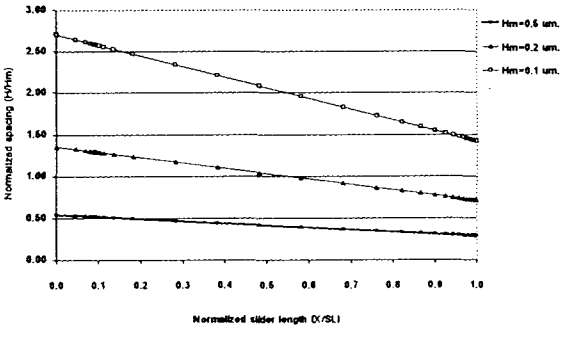

Pitch angle=0.0001 radian

Fig.4 Normalized flying height along slider rail

The effect of disk speed on clearance is presented on Fig.5.It seen that the increased disk speed from 10 to 60 m/s cause the minimum film thickness increased.

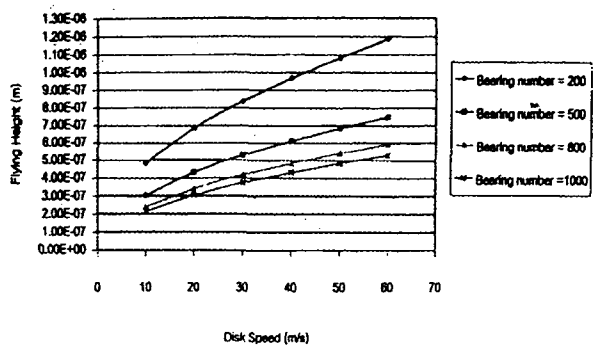

Fig. 5 Effect of disk speed on flying height

4.1.3 Load suspension

The load carrying capacity is presented on Fig.6.It is shown the increased disk speed from 5 to 30 m/s causes the load carrying capacity increase. Therefore, he required load suspension on slider head increase in order to maintain the slider inequilibrium.

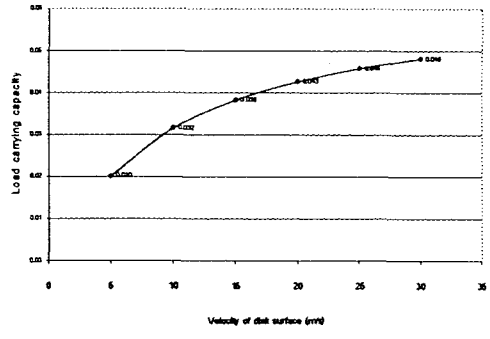

Fig. 6 Effect of disk speed on load carrying capacity

4.1.4 Pivot position

The pivot coordinate is moved far away form the middle point along the slider length when the disk speed increase as shown in Fig.7

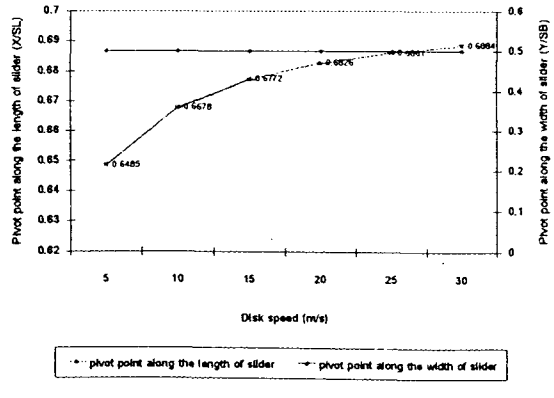

Fig. 7 Effect of disk speed on pivot coordinate point

4.2 Dynamic characteristics

Dynamic characteristics of air film with fixed configulation, air film stiffness and damping coefficient of the fixed air film configulation are first analyzed using the linearized analysis in the frequency domain to determine the fundamental dynamic characteristics of slider.

Figure 8 shows the air film stiffness and damping coefficients and normalized frequency $(= \omega / \omega_0)$ with varying the minimum flying height of slider. Figure 8(a) shows the stiffness K_{11} is positive valve and nearly constant in that frequency range and compare with varying minimum air film thickness .The stiffness coefficient decreased with minimum clearance decreased. Similary, the damping coefficient as shown in Fig.8 (b) decrease when the nondimensional frequency in this range is increase. In contrast to the stiffness coefficient K_{12} as shown on Fig.8(c) and damping coefficient C_{12} as shown on Fig.8(d) have negative value.

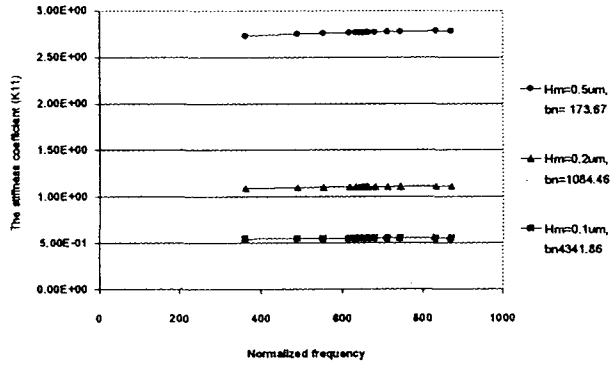

Fig. 8(a) Nondimensional frequency and K_{11}

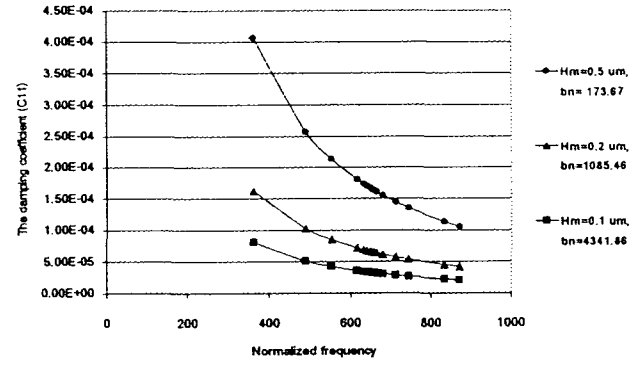

Fig. 8 (b) Nondimensional frequency and C_{11}

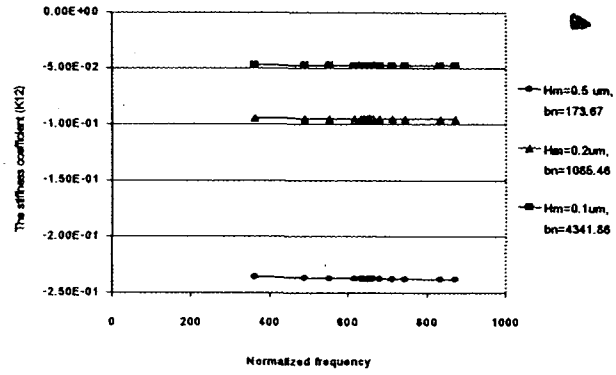

Fig. 8 (c) Nondimensional frequency and K_{12}

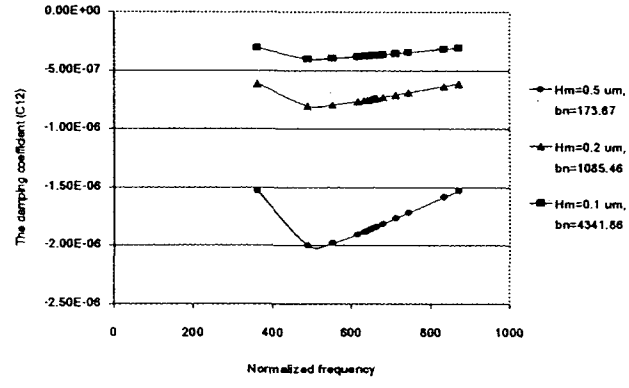

Fig. 8 (d) Nondimensional frequency and C_{12}

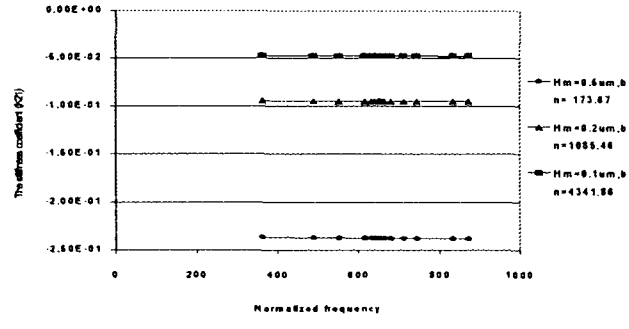

Fig. 8 (e) Nondimensional frequency and K_{21}

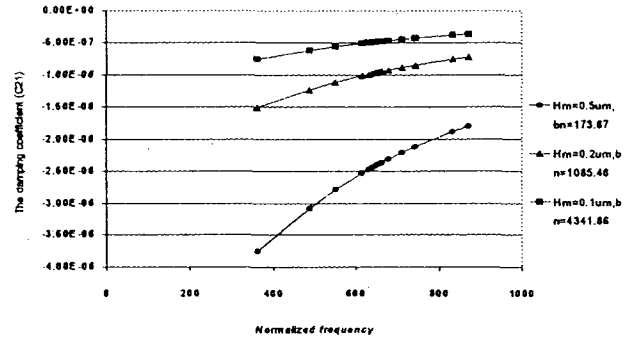

Fig. 8 (f) Nondimensional frequency and C_{21}

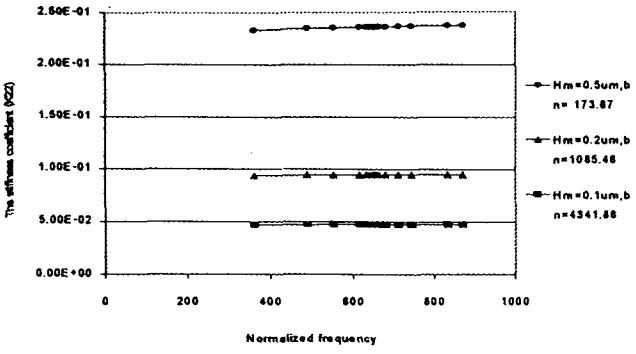

Fig. 8 (g) Nondimensional frequency and K_{22}

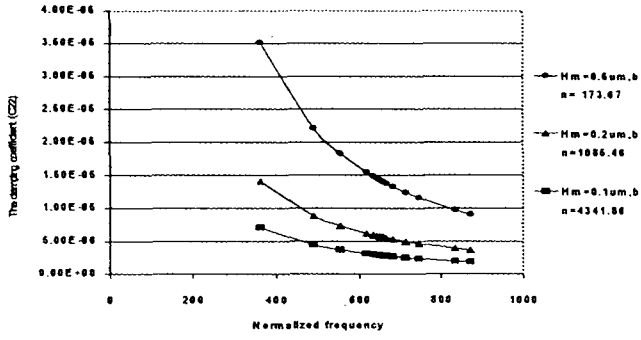

Fig. 8 (h) Nondimensional frequency and C_{22}

Fig. 8 Relationship between air film stiffness and damping coefficient and normalized frequency with vary bearing number and disk speed (U)=10 m/s

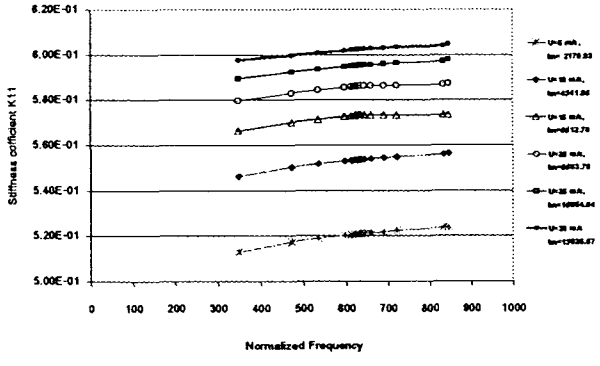

Fig. 9(a) Effect of disk speed on air film stiffness, K_{11}

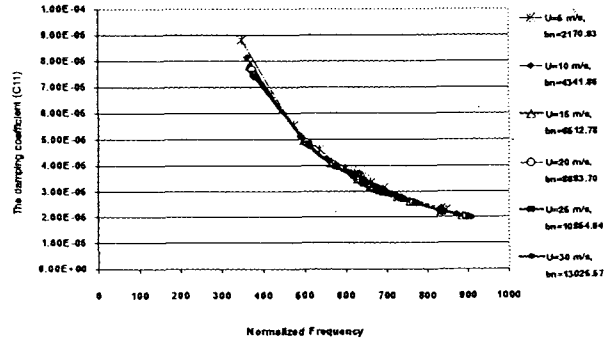

Fig. 9(b) Effect of disk speed on air film damping, C_{11}

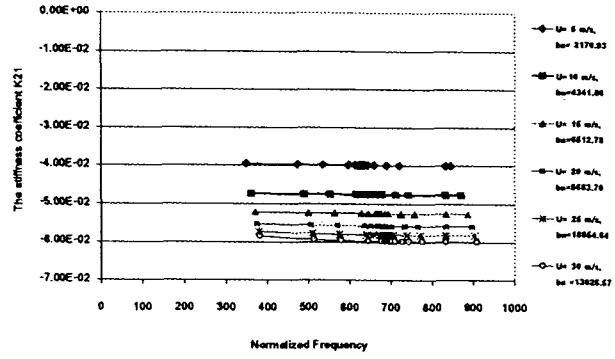

Fig. 9(c) Effect of disk speed on stiffness coefficient, K_{21}

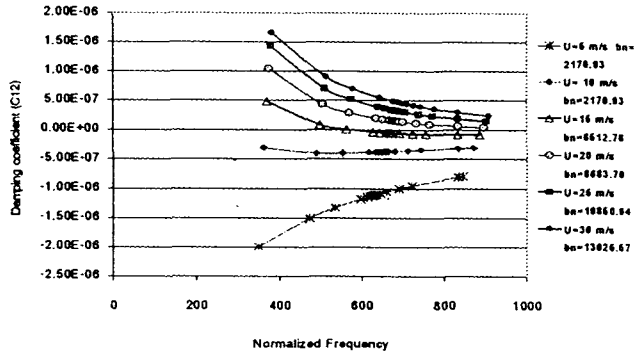

Fig. 9(d) Effect of disk speed on stiffness coefficient, C_{12}

Fig. 9 Relationship between air film stiffness and damping coefficient and normalized frequency with vary disk speed and minimum film thickness

Effect of disk speed on the air film stiffness and damping coefficient is presented on Fig. 9 .It shows the stiffness and damping coefficient with varying disk speed for minimum air film thickness of 0.1 μ m. Form Fig.9(d) we can see that the higher bearing number, the higher the damping coefficient can get. but it will decrease when the normalized frequency is increase.

The stiffness coefficient K_{11} (Fig.8 (a)) and K_{22} (Fig.8 (g)) are positive values. The stiffness K_{12} (Fig.8(c)) and K_{22} (Fig.8(e)) are negative values. The trend of those values are similary. Also the damping coefficient are follow this same manner too. The damping C_{11} (Fig.8 (b)) and C_{22} (Fig.8 (h)) are positive values. The damping C_{12} (Fig.8 (d)) and C_{21} (Fig. 8 (f)) are negative value. For the ultra low minimum spacing causes the stiffness and damping are low positive value and low negative value.

5.Conclusion

The static and dynamic characteristics of the air bearing head on a smooth rigid disk were investigated theoretically. The Finite difference method is used to solve the modified Reynolds

equation and linearized by Taylor's series to obtain pressure distribution and relationship between flying height and sliding velocity of rigid disk in the plane wedge-type slider in hard disk drive system. Similary, Laplace transformation has been applied to linearied time dependent modified Reynolds equation to obtain dynamic characteristics.

References

[1] Ellis Cha and D.B. Bogy," A Numerical Scheme for Static and Dynamic Simulation of Subambient Pressure Shaped Rail Sliders", Trans. ASME. Journal of Tribology, Vol. 105, 1995, pp. 36-46.

[2] J.W.White, "Flying Characteristics of Zero-Load Slider Bearing". Trans. ASME. Journal of Lubrication Technology, Vol. 105, 1983, pp.484-490.

[3] K. Kogure, S. Fukui, Y. Mitsuya and R. Kaneko," Design of Negative Pressure Slider for magnetic Recording Disks", Trans. ASME. Journal of Lubrication Technology, Vol. 105, 1983, pp.496-502.

[4] K. Ono, " Dynamic Charateristics of Air-Lubricated Slider Bearing Bearing for Non contact Magnetic Recording", Trans.ASME, Journal of Lubrication Technology, Vol.97, 1975, pp. 250-260.

[5] O.J. Ruiz and D.B. Bogy," A Numerical Simulation of the Head-Disk Assembly in Magnetic Hard Disk Files: Part I-Component Models", Trans. ASME. Journal of Lubrication Technology, Vol.112, 1990, pp. 593-602.

[6] T. Hayashi, S.Fukui, T.Ohkubo and R. Kaneko, " Dynamic Characteristics of Gas-Lubricated Slider Bearings Under High Knudsen Number Conditions ", Trans. ASME, Journal of Tribology, Vol.112, 1990, pp.111-118.

[7] T.G.Jeong and D.B.Bogy, 1993, " Numerical Simulation of Dynamic Loading in Hard Disk Drives", Trans. ASME, Journal of Tribology, Vol.115, 1993, pp. 370-375.